SEARCHES FOR SUPERSYMMETRY IN ATLAS*

Pawel Brückman de Renstrom

on behalf of the ATLAS Collaboration

The H. Niewodniczański Institute of Nuclear Physics PAN
Radzikowskiego 152, 31-342 Kraków, Poland

(Received April 19, 2010)

The boson–fermion unification offered by Supersymmetry is capable of providing remedies for various theoretical deficiencies of the experimentally established Standard Model. The Dark Matter candidate provided by a neutral Lightest Supersymmetric Particle is a prominent example. In the following we review the potential of the ATLAS experiment at the LHC to discover the most commonly considered R-parity conserving Supersymmetric scenarios, notably the mSUGRA and the GMSB models.

PACS numbers: 11.30.Pb, 98.80.Cq, 13.85.–t

1. Introduction

The postulate of a fundamental symmetry between bosonic and fermionic degrees of freedom offers solutions to a number of problems unresolved within the Standard Model (SM) of particle physics: Higgs mass fine tuning, unification of running coupling constants, candidate for the cosmological Dark Matter, to name just a few. Offering all that it remains highly predictive (at least in its minimal incarnation). The most relevant aspect in the context of this conference is admittedly the existence of the Dark Matter (DM) candidate thanks to the R-parity conservation. This, however, puts constraints on Supersymmertic models themselves. The Lightest Supersymmetric Particle (LSP) must be weakly interacting and neutral. If realized by nature, Supersymmetry (SUSY) must be a broken symmetry. Direct experimental evidence for superpartners has not been reported. The Supersymmetry breaking mechanism has implications for the low energy scale physics [1]. The minimal model with gravity mediated SUSY breaking (mSUGRA) appears among the most popular scenarios with the lightest neutralino as the

* Presented at the Cracow Epiphany Conference on Physics in Underground Laboratories and Its Connection with LHC, Cracow, Poland, January 5–8, 2010.

LSP[1]. This model does not preclude the possibility of direct detection of weakly interacting massive particles (WIMP) by terrestrial experiments. In contrast, the gauge mediated SUSY breaking model (GMSB) being an interesting alternative with gravitino LSP and the lightest neutralino or a sfermion (usually stau) next to lightest Supersymmetric particle (NLSP) provides no possibility of direct WIMP detection due to very low cross-sections. Other scenarios like split SUSY leading to the possibility of producing long-lived R-hadrons, AMSB, NUHM are also considered in ATLAS but will not be covered here.

Results presented here have been obtained in the framework of the final assessment of the ATLAS physics potential [2] and are normalized to the LHC integrated luminosity of 1 fb^{-1} at the center of mass (CM) energy of 14 TeV.

2. Generic SUSY signatures and search strategy in ATLAS

At the LHC Supersymmetry is produced preferentially via strong interactions due to their large cross-section. In R-parity conserving SUSY models supersymmetric particles are always pair-produced and at the end of both decay cascades a stable LSP must remain. Cosmology requires that the LSP is neutral and weakly interacting, hence escaping detection and leading to sizable missing transverse energy ($\not{E}_{\mathrm{T}}$) in the event. Cascades with the escaping LSP preclude observation of any sparticle mass resonances. Decays of SUSY particles produced at the primary interaction usually involve long cascades which lead to multiple jets and isolated leptons in the final state. Such events are characterized by large M_{eff}[2] and larger transverse sphericity than most SM backgrounds.

Final states involving multiple jets imply large theoretical uncertainties on modeling of the SM backgrounds. These are mostly $t\bar{t}$ $W+$jets, $Z+$jets and the QCD. This is why data-driven methods for estimating SM backgrounds are of fundamental importance in searches for Supersymmetry at the LHC.

The most commonly studied mSUGRA model is parametrized by just five constants which uniquely determine the electroweak scale phenomenology. If cosmological constraints from the DM abundance are to be taken strictly the $m_0, m_{1/2}$ parameter space of mSUGRA is in its large part excluded [3]. The only allowed regions are those with enhanced annihilation or co-annihilation of light SUSY particles which could reduce the abundance of the supersymmetric component in the early Universe just before the freeze-out.

[1] In most of the parameter space.

[2] M_{eff} is defined as the scalar sum of transverse momenta of all selected jets, isolated leptons and the $\not{E}_{\mathrm{T}}$: $\mathrm{M_{eff}} \equiv \sum p_{\mathrm{T}}^{\mathrm{jet}} + \sum p_{\mathrm{T}}^{\mathrm{lep}} + \not{E}_{\mathrm{T}}$.

In ATLAS the choice of the SUSY benchmark points in the mSUGRA model was motivated by the cosmological constraints. Table I summarizes the points relevant for the following discussion[3]. Benchmark points SU1 and SU8.1 are two different variants of the Coannihilation region where $\tilde{\chi}_1^0$ annihilate with near-degenerate $\tilde{\ell}$. SU2 is the Focus region near the boundary where $\mu^2 < 0$. This is the only region in mSUGRA where the $\tilde{\chi}_1^0$ has a high higgsino component, thereby enhancing the annihilation cross-section for processes such as $\tilde{\chi}_1^0\tilde{\chi}_1^0 \to WW$. SU3 is the Bulk region point where LSP annihilation happens through the exchange of light sleptons. SU4 has been dubbed the Low mass point. It lies in the Bulk region but is characterized by the lowest allowed SUSY masses near to the Tevatron bound. Finally, SU6 is in the Funnel region where $2m_{\chi_1^0} \approx m_A$. Since $\tan\beta \gg 1$, the width of the pseudo-scalar Higgs boson A is large and decays to τ dominate.

TABLE I

Summary of the mSUGRA benchmark points chosen by ATLAS.

Point	M_0 [GeV]	$M_{1/2}$ [GeV]	A_0 [GeV]	$\tan\beta$	signμ	$\sigma_{\rm LO}$ [pb]
SU1	70	350	0	10	+	8.15
SU2	3550	300	0	10	+	5.17
SU3	100	300	−300	6	+	20.85
SU4	200	160	−400	10	+	294.46
SU6	320	375	0	50	+	4.47
SU8.1	210	360	0	40	+	6.48

Cross-sections for the SUSY signal benchmark samples were calculated at the NLO using the PROSPINO 2.0.6 program [4] and CTEQ6M [5] PDF functions. After generation events were passed through the full simulation of the ATLAS detector. The same procedure was used for generating GMSB signal samples featuring different NLSP identity, mass and lifetime scenarios. The fully simulated benchmark samples were used for detailed understanding of signal selection criteria. Nonetheless, the full scan of the mSUGRA parameter space was not limited to the cosmologically allowed regions. Only the direct exclusion limits from LEP [6] and Tevatron [7, 8] were respected. The scan was performed using signal samples simulated with the fast detector simulation (ATLFAST [9]) and using LO cross-sections which renders all the derived discovery limits conservative. Signal significance (Z_n) was obtained by the convolution of a Poisson distribution representing statistical fluctuation and a Gaussian for the systematic uncertainty:

[3] The convention of $c \equiv 1$, hence same units for energy, momentum and mass, will be used hereafter.

$$Z_n = \sqrt{2}\,\mathrm{erf}^{-1}(1-2p)\,, \quad \text{where} \quad p \propto \int_0^\infty d\,b\,G(b;N_b,\delta N_b) \sum_{i=N_{\mathrm{data}}}^{\infty} \frac{e^{-b}b^i}{i!}\,. \tag{1}$$

Significances were always corrected for multiple trials[4]. All SM backgrounds were generated using either NLO Monte Carlo (MC@NLO for $t\bar{t}$) or LO Monte Carlo renormalized and to NLO (NNLO for W and Z), then fully simulated and reconstructed in ATLAS. A variety of data-driven techniques to estimates SM background rates were identified and studied as described in Section 4.2. Nonetheless, conservative systematic uncertainties on the overall normalization of the backgrounds were assumed (20% for W + jets, Z + jets and $t\bar{t}$, 50% for QCD).

3. The ATLAS detector at the LHC

The LHC accelerating complex is designed to collide proton on proton beams with the CM energy of 14 TeV and instantaneous luminosity of 10^{34} cm^{-2}s^{-1} (10 nb^{-1}s^{-1}). LHC bunches spaced by 25 ns will contain $\approx 10^{11}$ protons each. In the initial phase, however, it is planned to operate the LHC at a reduced CM energy and beam intensities. In years 2010 and 2011 LHC is scheduled to operate at 7 TeV CM energy and deliver 1 fb^{-1} of integrated luminosity per experiment. Only a small fraction of this statistics can be expected in 2010 alone.

ATLAS [10] is one of the two general purpose experiments at the LHC providing tracking, particle identification and hermetic calorimetry in the 4π solid angle. Charged particle tracking is provided by the Inner Detector (ID) covering the pseudorapidity range $|\eta| < 2.5$ and immersed in the solenoidal magnetic field of 2T. Looking from inside out, the ID consists of three subsystems: the silicon Pixel Detector, the silicon strip detector (SCT) and the straw drift tube tracking device (TRT). The latter is equipped with an additional radiator allowing for e/π separation via detection of transition radiation. Overall, the ID provides highly efficient and precise tracking over the full pseudorapidity coverage with the momentum resolution of $\sigma/p_{\mathrm{T}} \sim 3.4 \times 10^{-4} \times p_{\mathrm{T}}$ (GeV) $\oplus$ 0.015. ATLAS is equipped with Pb-LAr accordion electromagnetic calorimeters with e/γ identification and triggering capabilities and energy resolution of $\sim$ 1% at 100 GeV and 0.5% at 1 TeV. These are surrounded with the Fe/scintillator (central region) and Cu/W/LAr (forward regions) hadronic calorimeters. They provide hermetic-

[4] Signal significance was looked at in multiple statistically independent samples and using various techniques. Assumed statistical fluctuations accounted for this fact.

ity, trigger, jet reconstruction and missing transverse energy ($\not\!\!E_{\rm T}$) measurement down to $|\eta| < 5$ with energy resolution of $\sigma/E \sim 50\%/\sqrt{E} \oplus 0.03$. Muon trigger and muon momentum measurement with the resolution $< 10\%$ up to $E_\mu \approx 1$ TeV is assured by large air-core toroids with gas-based drift chambers covering the solid angle of $|\eta| < 2.7$ surrounding the calorimeter system. ATLAS features three levels of trigger (only first one being hardware-based) which reduces the initial 40 MHz rate of bunch crossing down to ~ 200 Hz of interesting physics events that can be recorded.

4. mSUGRA motivated searches

The ATLAS search strategy was structured according to the possible final state signatures.

4.1. Final state modes for SUSY discovery

The inclusive signatures considered were: 4 jets and no leptons, 4 jets + one lepton, 2 (or 3) jets with 0 or one lepton, 4 jets + 2 leptons (opposite or same sign), 3 leptons + jet and exclusive 3 leptons with $\not\!\!E_{\rm T}$. Additionally, signatures with 4 jets with either a reconstructed tau lepton or with two jets tagged as originating from a b quark were considered as these should be enhanced at high value of $\tan\beta$. In the following, only selected examples will be discussed.

The 4 jets with no leptons analysis required at least four reconstructed jets with $p_{\rm T} > 50$ GeV, one with $p_{\rm T} > 100$ GeV, event missing transverse energy satisfying both $\not\!\!E_{\rm T} > 100$ GeV and $\not\!\!E_{\rm T} > 0.2{\rm M}_{\rm eff}$. QCD background was additionally reduced requiring transverse sphericity[5] $S_{\rm T} > 0.2$. Events containing an isolated muon or electron were explicitly vetoed. The trigger requiring a jet with $E_{\rm T} > 70$ GeV and $\not\!\!E_{\rm T} > 70$ GeV was found to be over 90% efficient for this mode. The channel benefits from the highest statistics but retains sizable contribution of the QCD background. Figure 1 shows the $M_{\rm eff}$ distributions after the cuts listed above. On the left there is the resulting composition of backgrounds compared to the SU3 signal and on the right the expected signal from the different mSUGRA benchmark points on top of the SM background. The plots justify the final selection cut requiring ${\rm M}_{\rm eff} > 800$ GeV. Only the SU2 benchmark (Focus Point model) is not accessible in this channel. Due to very high masses of sfermions only gluinos can be strongly produced and the decay cascades contain fewer energetic jets. Leptonic signatures are more promising in this corner of the parameter space.

[5] Transverse sphericity is defined as $S_{\rm T} \equiv \frac{2\lambda_2}{(\lambda_1+\lambda_2)}$ where λ are the eigenvalues of the momentum tensor in the transverse plane $S_{ij} = \sum_k p_{ki} p^{kj}$.

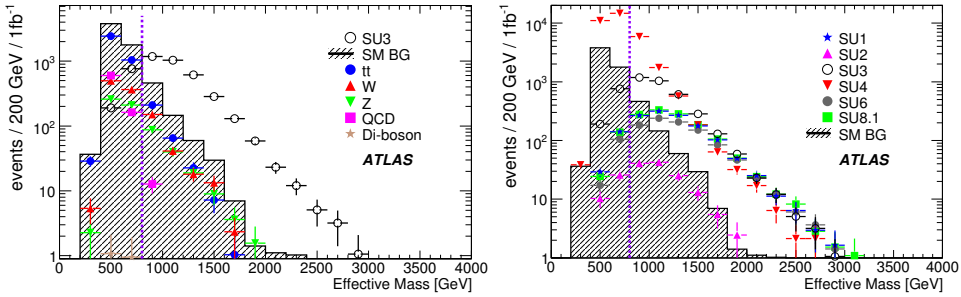

Fig. 1. Effective mass (M_{eff}) distributions after all cuts in the 0-lepton mode (except the cut on M_{eff}) for SM backgrounds and SUSY SU3 point (left), total Standard Model background and various mSUGRA benchmark points (right). The vertical line indicates the final selection cut: $\text{M}_{\text{eff}} > 800$ GeV.

Selection of 4 jets plus one lepton mode used similar criteria except exactly one lepton with $p_{\text{T}} > 20$GeV and no other leptons with $p_{\text{T}} > 10$GeV was required. Additionally, the transverse mass of the lepton plus the $\not{E}_{\text{T}}$ system (M_{T}) was required to exceed 100 GeV. Figure 2 shows the M_{eff} distribution for the mSUGRA benchmark points and the total Standard Model background. The latter is by far dominated by $t\bar{t}$. A similar pattern as in the case of the 4-jets plus zero leptons is apparent. Most of the benchmark points show similar behavior apart from the Low mass point which is massively enhanced for the low M_{eff} values and the Focus Point model which has much smaller significance over the whole M_{eff} range.

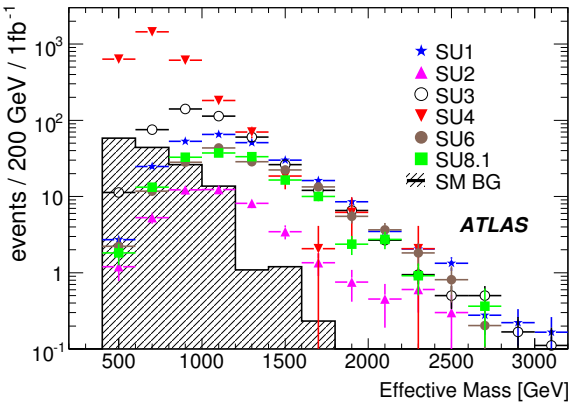

Fig. 2. Effective mass (M_{eff}) distributions after all cuts in the 1-lepton mode (except the cut on M_{eff}). The shaded histogram is the total SM background and various mSUGRA benchmark points are given by polymarkers with errors.

It should be noted that the Supersymmetric signal generically includes lower jet multiplicity final states resulting *e.g.* from a direct squark decay to a gaugino. Lower jet multiplicity may be attractive especially for the early data, where understanding of topologically complicated events may be limited. Systematic uncertainties on modeling of multi-parton final states are generally large. ATLAS studied its SUSY discovery potential in the inclusive channels with two or three jets only. Naturally higher Standard Model background had to be compensated by harder cuts on jet energy and $\not{E}_{\mathrm{T}}$. In the 2-jet analysis cuts were modified to require at least two jets with $p_{\mathrm{T}} > 100$ GeV and one with $p_{\mathrm{T}} > 150$ GeV. The requirement on the missing transverse energy was raised to $\not{E}_{\mathrm{T}} > 0.3\mathrm{M}_{\mathrm{eff}}$. The approach proved efficient in both 0 and 1 lepton modes leading to a competitive discovery reach. Figure 3 shows the M_{eff} distributions after all cuts resulting from the 2-jet selection. On the left the expected signal from the different mSUGRA benchmark points on top of the SM background for the 0-lepton mode. On the right there is the resulting composition of backgrounds compared to the SU3 signal for the 1-lepton channel. The final cut on $\mathrm{M}_{\mathrm{eff}} > 800$ GeV was applied in this variant of the selection as well.

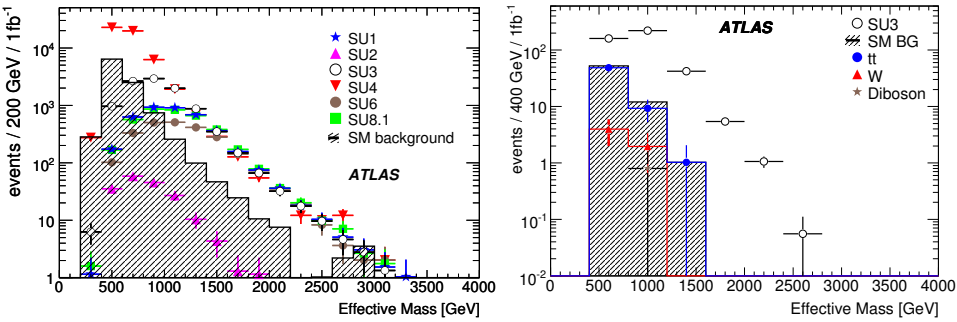

Fig. 3. Effective mass (M_{eff}) distributions after all cuts in the two jets + $\not{E}_{\mathrm{T}}$ mode (except the cut on M_{eff}). Left: total Standard Model background and various mSUGRA benchmark points in the 0-lepton channel. Right: SM backgrounds and SUSY SU3 point in the 1-lepton channel.

The baseline analyses involving two or three isolated lepton candidates will not be discussed here. They are all documented in detail in [2]. Here let us only have a closer look at so-called "worst case scenario", where in the Focus Point model characterized by a very high m_0 we additionally assume that strong SUSY production through gluinos is suppressed. In such a scenario SUSY signal can be identified by three isolated leptons in the final state. The cross-section for the direct gaugino production with the decay to three leptons is small (≈ 32.6 fb). Additionally, this channel is difficult due to low mass differences between the gauginos hence low p_{T} of the final state leptons

and low $\not{E}_{\mathrm{T}}$. Signal selection required three leptons with $p_{\mathrm{T}} > 10$ GeV out of which two make the same flavor and opposite sign (SFOS) pair. In order to suppress Standard Model backgrounds from WZ production and inclusive high p_{T} photons $\mathrm{M_{SFOS}} < 21.2$ GeV and $81.2\ \mathrm{GeV} < \mathrm{M_{SFOS}} < 101.2$ GeV were vetoed. The leptons were additionally required to be isolated from any hadronic activity. The track isolation was found to be the most efficient criterion. It consisted of a requirement that there was no track with p_{T} exceeding certain threshold in a given ΔR[6] cone around the lepton. ${p_{\mathrm{T}}^{\Delta R=0.2}}_{\mathrm{max}} < 2$ GeV for electrons and ${p_{\mathrm{T}}^{\Delta R=0.2}}_{\mathrm{max}} < 1$ GeV for muons was used. The cut on $\not{E}_{\mathrm{T}}$ had to be kept low. The optimal one was found at $\not{E}_{\mathrm{T}} > 30$ GeV. The Standard Model backgrounds to this channel are low but the stringent lepton isolation cuts were necessary to keep $t\bar{t}$ and Zb low. The WZ is an inherently irreducible background to this channel. The left plot in figure 4 shows the $\mathrm{M_{SFOS}}$ distributions for the SU2 direct

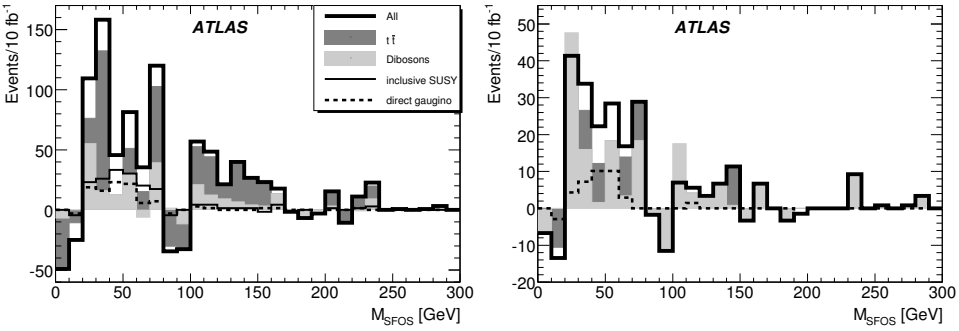

Fig. 4. Flavor subtracted (see text) mass of the same flavor opposite sign (SFOS) lepton pairs after all selection cuts (except the cut on $\mathrm{M_{SFOS}}$) for the SU2 benchmark point and direct gaugino production. No jet veto (left) and with the jet veto (right). The distributions are normalized to 10 fb^{-1}. Only the mass range of $21.2\ \mathrm{GeV} < \mathrm{M_{SFOS}} < 81.2$ GeV was used for the signal significance calculation.

gaugino production and the remaining Standard Model backgrounds after all described cuts. The distribution has been flavor subtracted, and the quantity plotted is $n^{\mathrm{SFOS}} - n^{\mathrm{DFOS}}$ where n^{DFOS} is the number of events in which there are three leptons, but no SFOS pair. The subtraction eliminates contributions from the flavor uncorrelated backgrounds. Due to very low cross-sections the plot has been normalized to 10 fb^{-1}. The right plot shows the same distribution after an additional veto on jets exceeding 20 GeV. This reduced significantly the $t\bar{t}$ background. Although the systematic error on this channel is small ($\approx 5\%$), SUSY discovery in this particularly

[6] $\Delta R \equiv \sqrt{\Delta\phi^2 + \Delta\eta^2}$.

difficult corner of the parameter space requires considerably larger $L_{\rm int}$. The 5σ discovery would be possible with the integrated luminosity in excess of 80 fb^{-1}.

4.2. Data driven methods of background estimation

Due to a lack of distinct resonances in the Supersymmetric signal, understanding of the Standard Model background rates is of prime importance. They must eventually be measured from data. This includes understanding of the detector response (efficiencies, jet energy scale, $\not\!\!E_{\rm T}$, *etc.*) as well as estimation of final background rates to individual search channels. A large collection of techniques to estimate various backgrounds to different final state signatures have been put in place by the ATLAS Collaboration [2]. Here let us quote merely a few examples.

Detector response to jets can be studied using two different techniques. Resolution on the bulk of the distribution can be measured from the transverse energy balance in the events where a jet recoils against a photon. Due to lack of statistics this technique cannot be used to measure the non-Gaussian part in the far tail. This, in turn, can be assessed via the jet mismeasurements in the QCD 3-jet events. The jet collinear with a sizable $\not\!\!E_{\rm T}$ is considered to have fluctuated in its measured energy.

Multiple background estimation techniques rely on identifying two selection variables approximately uncorrelated in the background. Each of them must be able to identify a signal-rich and signal-suppressed control region, thus dividing the phase-space into four regions (let us call them A, B, C and D). If D is signal-rich, the background rate in this region can be estimated from $n_{\rm D} = n_{\rm C} \times n_{\rm B}/n_{\rm A}$. The estimate would be exact if signal was absent in the A, B and C control regions. In reality this is true only if there is no signal in data. Otherwise, further corrections must be applied. *E.g.* the technique dubbed "new $M_{\rm T}$" proved effective in the one-lepton channel. It used re-iteration of the above procedure correcting for the signal contribution to the control regions. The latter was obtained using its initial estimate and $M_{\rm T}$ signal distribution from the Monte Carlo. An example of the "new $M_{\rm T}$" method is demonstrated in figure 5. It shows the total Standard Model background to the 4-jet + one lepton channel in the $\not\!\!E_{\rm T}$ (left) and the $M_{\rm eff}$ (right) views. The transverse mass of the lepton and the $\not\!\!E_{\rm T}$ system ($M_{\rm T}$) and the $\not\!\!E_{\rm T}$ were used as the discriminating variables. SUSY suppressed control region (C) was defined by $\rm M_T < 100$ GeV while 100 GeV $< \not\!\!E_{\rm T} <$ 150 GeV was used for the normalization (B/A). Plots show a satisfactory performance of the iterative method even in the presence of a strong SUSY signal.

A complementary method is provided by the so called "tiles method" [11]. It also uses two selection variables to divide the phase-space in four regions. In this method, however, Standard Model backgrounds may exhibit

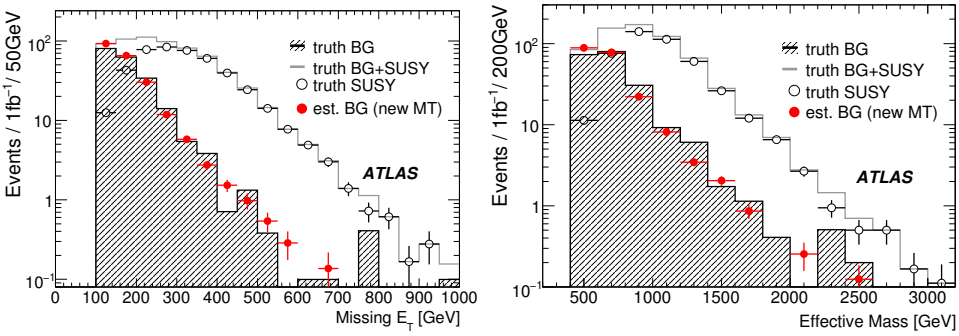

Fig. 5. $\not{E}_{\mathrm{T}}$ (left) and M_{eff} (right) distributions for the 1-lepton channel. Shaded histograms is the Standard Model background and closed points represent its estimate using the "new M_{T} method". Open circles show the SUSY signal present in the sample.

correlations in these two variables. In turn, they are required to be quasi-independent in the signal. If background fractions in the four regions are known from the Monte Carlo the system of linear equations can be solved exactly yielding the number of signal and background events in the signal-rich region.

Finally, let us recall a technique dedicated to the estimation of the important Standard Model background to the 0-lepton mode: the $Z \to \nu\nu$+jets. It uses the standard 0-lepton signal selection with an additional requirement of a $Z \to l^+l^-$ candidate. $p_{\mathrm{T}}(l^+l^-)$ is then substituted for the $\not{E}_{\mathrm{T}}$. Figure 6 shows the comparison between the true and the estimated $Z \to \nu\nu$+jets background in the $\not{E}_{\mathrm{T}}$ (left) and the M_{eff} (right) views. The appropriate acceptance (η, p_{T}), efficiency and branching fraction corrections have been applied.

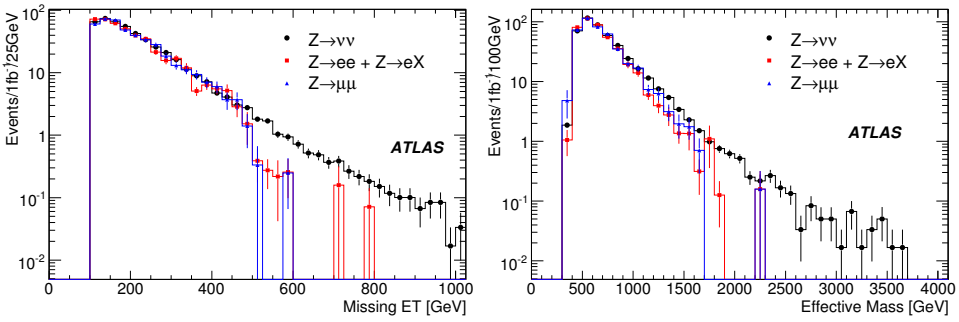

Fig. 6. $\not{E}_{\mathrm{T}}$ (left) and M_{eff} (right) distributions for the genuine $Z \to \nu\nu$ and its estimations based on $Z \to l^+l^-$.

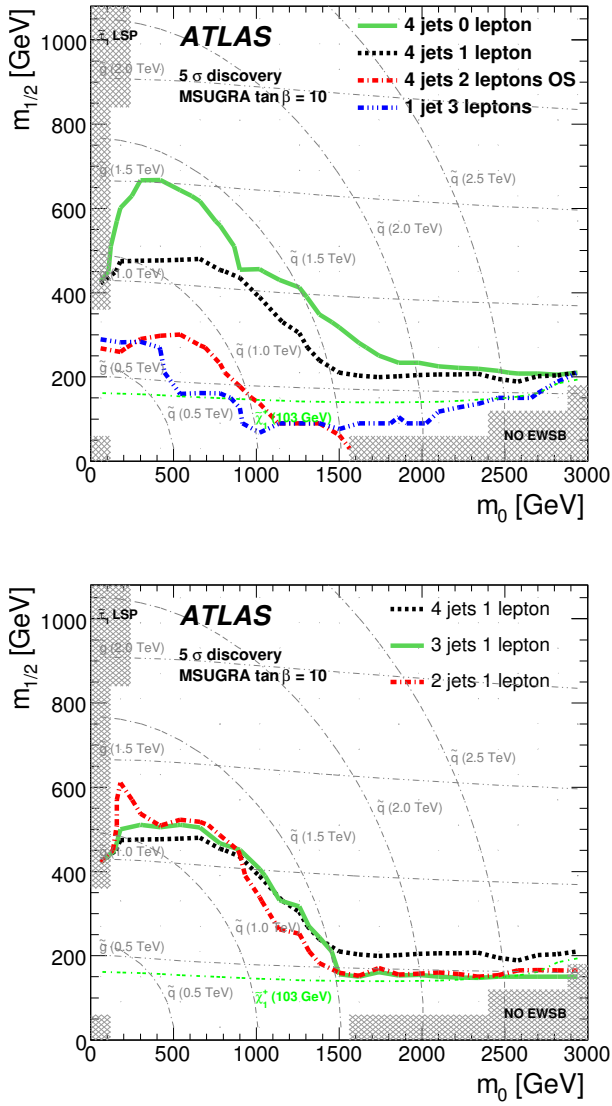

Fig. 7. $m_0, m_{1/2}$ contours of 5σ discovery for mSUGRA scenario at $\tan\beta = 10$ and $L_{\text{int}} = 1\,\text{fb}^{-1}$. Top: baseline signatures including either 4 jets and different number of leptons or one jet and 3 leptons. Bottom: comparison of discovery potentials between one lepton channels with different requirement on jet multiplicity (1, 2 or 3).

4.3. Summary of the discovery potential

In the above we have shown examples of selected inclusive SUSY searches motivated by the mSUGRA phenomenology. They were established using

fully simulated samples of the SUSY signal for the chosen benchmark points as well as the Standard Model background. The discovery potential in the allowed mSUGRA parameter space was ultimately estimated using a full grid scan and fast simulation as described in Section 2. Figure 7 shows the 5σ discovery contours on the $m_0, m_{1/2}$ plane for $\tan\beta = 10$ and integrated luminosity of 1 fb^{-1}. Already this moderate luminosity spectacularly extends the current reach of the Tevatron [7, 8]. The left plot shows the discovery contours for the analysis involving 4-jets plus various number of leptons and the 3-lepton plus a jet. Not surprisingly, the lepton-based one becomes competitive in the Focus region of the parameter space. On the right a comparison of one-lepton plus different jet multiplicity analysis demonstrates that the lower jet multiplicity modes lead to closely competitive significances.

5. Searches for the GMSB signatures

mSUGRA is merely a convenient framework for assessing the discovery potential for R-conserving SUSY with $\tilde{\chi}_1^0$ as the LSP. Other SUSY breaking scenarios lead to different electroweak-scale phenomenologies.

In the following we will briefly discuss possibility of SUSY discovery in the GMSB scenarios with the gravitino LSP. We consider two possibilities of either $\tilde{\chi}_1^0$ NLSP which decays to the $\tilde{G}$ emitting a hard photon or meta-stable slepton NLSP, usually a $\tilde{\tau}$. Table II summarizes the chosen benchmark points for the $\tilde{\chi}_1^0$ NLSP case. The lifetime of the $\tilde{\chi}_1^0$ NLSP is proportional to the C_G^2 parameter. The corresponding lifetimes are given in the table. GMSB1 leads to high p_{T} photons pointing back to the interaction point. The other two points result in so called "non-pointing" photons due to large decay length of the $\tilde{\chi}_1^0$.

TABLE II

Summary of the neutralino NLSP samples. Dataset GMSB1 is a prompt photon decay sample, while dataset GMSB2 and GMSB3 are the non-pointing photon samples. $N_5 = 1$, $\tan\beta = 5$, $\mathrm{sgn}(\mu) = +$ are used at each point.

Name	NLO (LO) σ [pb]	Λ [TeV]	M_m [TeV]	C_G	$c\tau$ [mm]	$M_{\tilde{\chi}}$ [GeV]
GMSB1	7.8 (5.1)	90	500	1.0	1.1	118.8
GMSB2	7.8 (5.1)	90	500	30.0	9.5×10^2	118.8
GMSB3	7.8 (5.1)	90	500	55.0	3.2×10^3	118.8

Table III gives the parameters chosen for the GMSB5 point where $\tilde{\tau}$ NLSP is meta-stable and is assumed not to decay inside the detector.

The GMSB1–GMSB3 signal selection relies on detection of at least two isolated photons with $p_{\mathrm{T}} > 20$GeV. Additionally, the typical SUSY signa-

TABLE III

Summary of the slepton NLSP sample. $N_5 = 3$, $\tan\beta = 5$, $\mathrm{sgn}(\mu) = +$, and no decay of slepton is assumed.

Name	NLO (LO) σ [pb]	Λ [TeV]	M_m [TeV]	$M_{\tilde{\tau}}$ [GeV]
GMSB5	21.0 (15.5)	30	250	102.3

ture is required: ≥ 4 jets with $p_{\mathrm{T}} > 50$ GeV including at least one with $p_{\mathrm{T}} > 100$ GeV, $\not{E}_{\mathrm{T}} > 100$ GeV & $\not{E}_{\mathrm{T}} > 0.2\mathrm{M}_{\mathrm{eff}}$. The trigger requiring either a photon above 55 GeV or two isolated photons above 17 GeV was assumed in this analysis. The GMSB1 signal and the remaining Standard Model background after all described cuts is shown on the left plot in figure 8. The requirement of two reconstructed photons results in almost pure signal in the sample. Even with a moderate integrated luminosity of 1 fb^{-1} we can either discover or exclude this GMSB scenario up to high sparticle masses. $\Lambda = 100$ TeV corresponds to squark and gluino masses in excess of 3 TeV. Additionally, a measurement of the $\tilde{\chi}_1^0$ lifetime is possible in this channel. It can be done either by measuring the photon flight direction via reconstruction of the calorimeter cluster centroids in the subsequent layers or using the precise calorimeter timing.

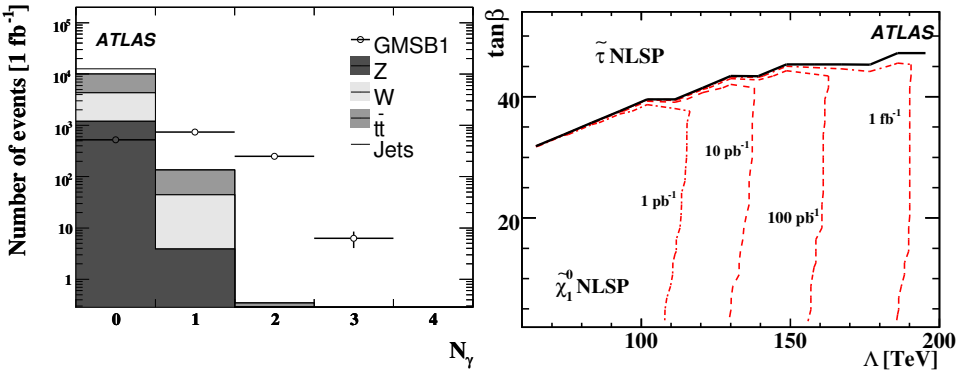

Fig. 8. Left: number of isolated photons in events after all selection cuts (except the one on N_γ). Shaded histograms are various Standard Model backgrounds while the open circles is the GMSB1 benchmark point signal. Right: The GMSB discovery reach on the $\Lambda, \tan\beta$ plane for different integrated luminosities.

In the GMSB5 the main signature is the high-p_{T} penetrating track with low β. The main technical challenge lies in the fact that the signal may be partly reconstructed inside the subsequent bunch crossing time window. Nonetheless, such a data acquisition mode is optionally foreseen in the ATLAS muon system. At Level 1 a standard muon trigger is required. At Level 2 of the trigger the 3 ns TOF resolution of the Resistive Plate Chambers can be fully exploited leading to the measurement of the particle velocity. The left plot in figure 9 shows the mass of the penetrating particle measured in the ATLAS muon system at the Level 2 of the trigger. The shaded histogram is the GMSB5 signal and open one the background from muons. The technique allows for signal selection already at the trigger level. Presented analysis required the reconstructed mass to be in excess of 40 GeV. The offline reconstruction of the slow moving GMSB sleptons presents another technical difficulty. Muon chambers are gaseous drift devices and their spacial resolution depends on the precise determination of the time of arrival (t_0). For particles with $\beta < 1$ t_0 is wrong. A dedicated track fitting technique has been developed whereby not only track parameters but also the particle velocity is optimized. In combination with the Level 2 trigger information this allows for a precise reconstruction of the candidate particle mass. The right plot in figure 9 demonstrates the expected resolution of the reconstructed invariant mass. A 102.3 GeV $\tilde{\tau}$ can be clearly distinguished from virtually massless muons.

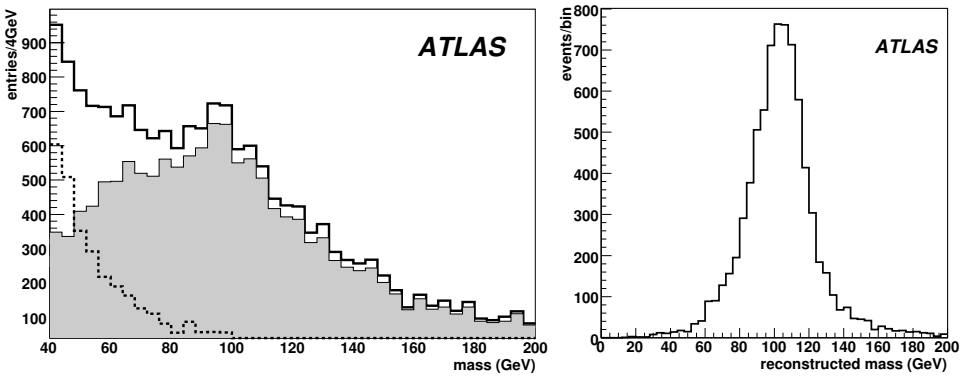

Fig. 9. Mass of the muon-like particle as measured from the time-of-flight by the L2 trigger (left) and reconstructed by the offline algorithms (right). The left plot shows the muon background from the Standard Model (dotted histogram) and the $\tilde{\tau}$ signal (shaded histogram). In the right plot only the GMSB5 $\tilde{\tau}$ signal is shown.

Nota bene, the same technique may be applicable to searches for R-hadrons [2].

6. Measurements from Supersymmetric events

If discovered, SUSY will have to be understood better. Inclusive signatures used for the generic searches may also result from other beyond Standard Model physics. We need more measurements to be able to confidently claim a Supersymmetric nature of the observed signal. One possibility comes from the measurement of the spin of superpartners as this is a distinct characteristic of Supersymmetry[7]. Another is the measurement of sparticle masses, more precisely of the relationships between them. Different SUSY breaking scenarios give precise predictions of the sparticle mass spectra at low energies. Mass values are not directly measurable, but various relationships may be deduced *e.g.* from observation of invariant mass edges.

Here let us only give an example of a measurement relating masses of the two lightest neutralinos: $\tilde{\chi}_2^0$ and $\tilde{\chi}_1^0$. The cascade decay may occur via the intermediate $\tilde{\ell}$ state, thus producing a same flavor and opposite sign lepton pair in the final state. The flavor subtracted[8] distributions of invariant mass of the lepton pair are shown in figure 10. The vertical lines indicate position of the edge to be measured. On the left is the distribution for the SU3 benchmark point where $m(\tilde{\chi}_2^0) > m(\tilde{\ell})$ while the right plot shows the distribution for the SU4 point where the mass hierarchy is reversed. The expression for the edge position is different in the two cases but is always uniquely determined by the masses of the neutralino states involved.

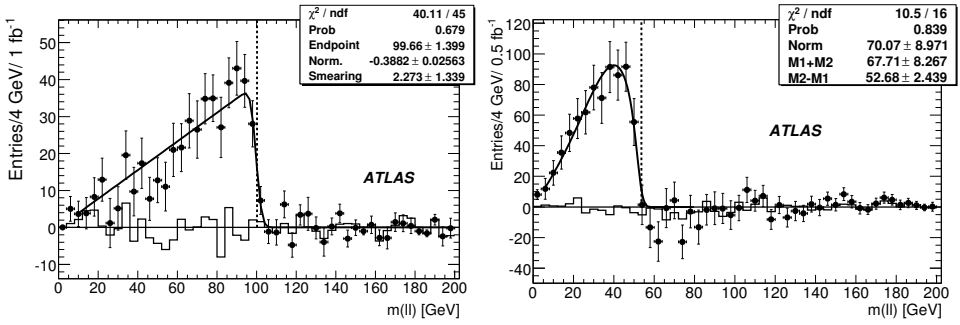

Fig. 10. The flavor-subtracted (see text) di-lepton mass distributions in the SU3 (left) and the SU4 (right) benchmark points. The mass edges are indicated with the dashed vertical lines. Plots are normalized to 1 fb^{-1} for the SU3 and 0.5 fb^{-1} for the SU4. The line histogram is the Standard Model contribution, while the points are the sum of Standard Model and SUSY contributions.

[7] Feasibility of spin determination via angular correlation of leptons emerging from the cascade has been demonstrated in ATLAS [2].

[8] Most SM backgrounds (*e.g.* $t\bar{t}$) lead to flavor uncorrelated lepton pairs. By subtracting different flavor sample from the same flavor sample (having corrected for the respective efficiencies) the background gets largely reduced.

Having performed measurements of multiple mass differences using various final states it is possible to do a global χ^2 fit to SUSY parameters. The procedure would yield the most likely SUSY scenario, hence the sparticle mass spectrum. These may further be converted into the cosmological Dark Matter abundance and compared to the expectation [12, 13].

Significant information discriminating Supersymmetry from other models and revealing its fundamental parameters can be extracted from data. Nonetheless, the complete picture would require a considerable amount of data, more that what can be expected in the first years of LHC running.

7. Conclusions

Supersymmetry breaking mechanism and the exact choice of parameters determine the electroweak scale phenomenology, hence the expected signatures from SUSY events. The ATLAS experiment performed detailed studies of its discovery potential over a wide range of models and parametrizations. In this report only example ones have been presented. The complete documentation can be looked up at the public page of the SUSY working group [14]. We reviewed briefly selected analyses motivated by the mSUGRA and GMSB model families which both assume exact R-parity conservation. This, in turn, is driven by the expectation of a Dark Matter candidate emerging from the model. A Supersymmetric LSP satisfies this requirement.

The results quoted here were obtained for the nominal center-of-mass energy of the LHC: 14 TeV and normalized to 1 fb^{-1}. In the years 2010–2011 LHC schedules operation at a reduced energy of 7 TeV. It is planned to collect 1 fb^{-1} per experiment by the end of this initial running period. Extrapolation of the derived discovery potential to lower energies is nontrivial as p–p cross-sections steeply fall especially for production of heavy objects. Not only the statistical significance is reduced but also important systematic uncertainties depend on the amount of collected data.

Last year an update to the studies discussed above was done for the scenario where the LHC would provide 200 pb^{-1} of data at 10 TeV over one year. The corresponding mSUGRA discovery limit contours are shown in figure 11. The left plot is for $\tan\beta = 10$ and the right one for $\tan\beta = 50$. Except for the small far Focus region the discovery is dominated by the 4-jets plus zero or one lepton analyses.

As a rule of thumb the drop of the LHC CM energy from 10 TeV to 7 TeV should reduce the statistical significances by roughly a factor of two. Accounting for five times larger L_{int} than assumed in the quoted result we end up at a similar ballpark estimate for SUSY discovery potential with data collected till the end of 2011 running.

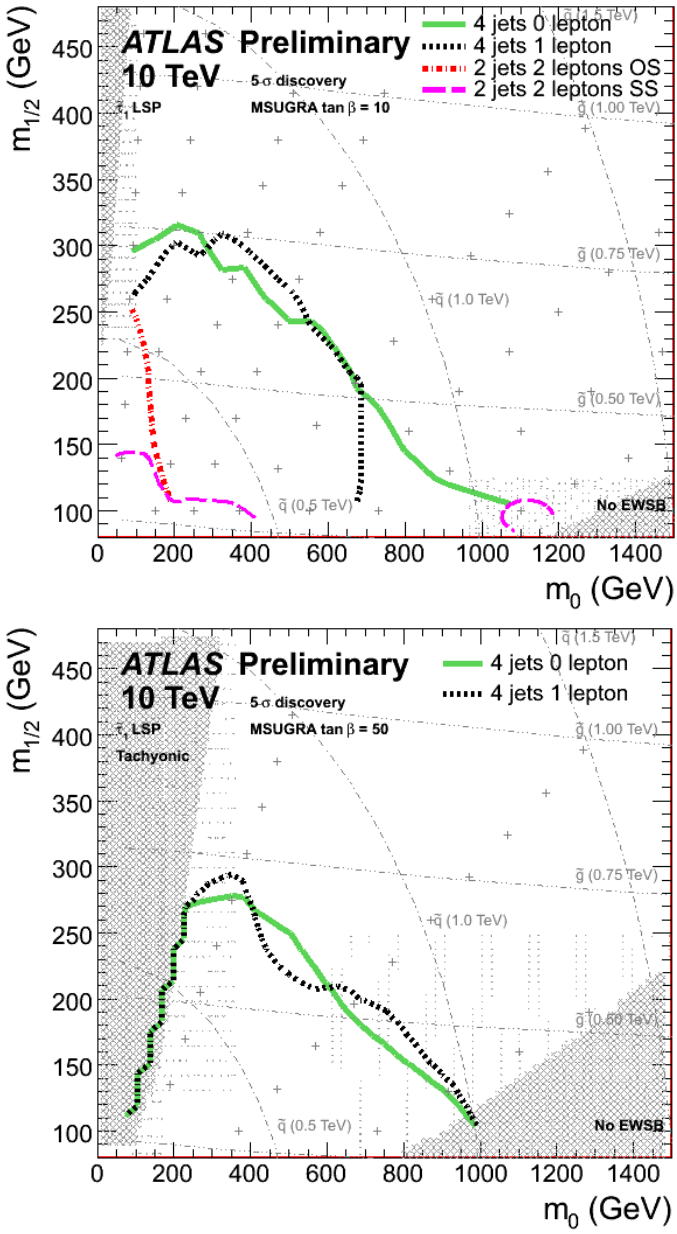

Fig. 11. $m_0, m_{1/2}$ contours of 5σ discovery for mSUGRA scenario at $\tan\beta = 10$ (top) and $\tan\beta = 50$ (bottom). Results are shown for the integrated luminosity of 200 pb^{-1} and center-of-mass collision energy of 10 TeV.

REFERENCES

[1] S.P. Martin, arXiv:hep-ph/9709356v5.

[2] ATLAS Collaboration, Expected Performance of the ATLAS Experiment, Detector, Trigger and Physics, CERN-OPEN-2008-020, Geneva 2008 and references therein.

[3] J.R. Ellis, K.A. Olive, Y. Santoso, V.C. Spanos, *Phys. Lett.* **B565**, 176 (2003) [arXiv:hep-ph/0303043].

[4] Prospino2, http://www.thphys.uni-heidelberg.de/~plehn/prospino/

[5] D. Stump *et al.*, *J. High Energy Phys.* **10**, 046 (2003).

[6] http://lepsusy.web.cern.ch/lepsusy/

[7] http://www-cdf.fnal.gov/physics/exotic/exotic.html

[8] http://www-d0.fnal.gov/Run2Physics/np/

[9] E. Richter-Was, D. Froidevaux, L. Poggioli, ATLFAST 2.0 a fast simulation package for ATLAS, ATL-PHYS-98-131.

[10] ATLAS Collaboration, *JINST* **3**, S08003 (2008).

[11] ATLAS Collaboration, Background Estimation for Inclusive SUSY Searches — The Tiles Method, ATL-PHYS-PUB-2009-077, 04 June 2009.

[12] G. Polesello, D.R. Tovey, *J. High Energy Phys.* **0405**, 071 (2004) [arXiv:hep-ph/0403047v2].

[13] M.M. Nojiri, G. Polesello, D.R. Tovey, *J. High Energy Phys.* **0603**, 063 (2006) [arXiv:hep-ph/0512204v1].

[14] https://twiki.cern.ch/twiki/bin/view/Atlas/SusyPublicResults